

**Coherent population trapping via a continuum with a train of ultrashort pulses**

Elena Kuznetsova,\* Roman Kolesov, and Olga Kocharovskaya  
*Department of Physics, Texas A&M University, College Station, Texas 77843-4242, USA*  
 (Received 22 March 2006; published 8 September 2006)

We consider the coherent population trapping effect with a train of ultrashort pulses in a  $\Lambda$ -type system with two bound states and a continuum replacing the upper state. Population transfer to the continuum can be totally suppressed provided that the splitting between the bound states is a multiple of the pulse repetition rate. Compared to the traditional case with only two laser fields coupling the bound states to the continuum, CPT with a pulse train allows one to avoid incoherent population losses due to interaction of the fields with “wrong” transitions, which results in only partial suppression of ionization. A method of suppression of excited-state absorption of pumping radiation in laser crystals, with pumping in the form of the pulse train, is proposed. As a particular example pumping dynamics of a  $\text{Ti}^{3+}:\text{YAlO}_3$  crystal using this technique is numerically analyzed.

DOI: [10.1103/PhysRevA.74.033804](https://doi.org/10.1103/PhysRevA.74.033804)

PACS number(s): 42.50.Gy, 32.80.Fb, 32.80.Qk

**I. INTRODUCTION**

Interaction of radiation with a quantum system containing a continuum, coupled by an optical field to some bound state(s), typically leads to unrecoverable loss of bound-state population. However, using coherent radiation the bound state-continuum interaction can be effectively controlled. A strong coherent laser field can admix the bound state to the continuum, forming a laser-induced continuum structure (LICS) [1], which can be probed by a second (weak) laser field, coupling the same continuum to another bound state. Tuning the probe field frequency an asymmetric ionization profile (first derived by Fano [2] for a continuum with an autoionizing state), can be detected, having regions of enhanced and suppressed ionization. Ionization suppression of as much as 70–80 % due to formation of the LICS and coherent population trapping (CPT) in bound states was reported in helium [3] and xenon [4]. Control over branching into different dissociative continua based on LICS was demonstrated in molecules [5], giving rise to coherent control of chemical reactions. Recently efficient coherent population transfer of about 6% of initial bound state population to a target bound state mediated by the continuum was demonstrated in the same helium system [6]. These results prove that the interference and coherence phenomena such as electromagnetically induced transparency (EIT) [7], CPT [8], slow light [9], coherent population transfer [10], typically considered in a system with three bound states forming a  $\Lambda$  configuration can be as well realized with some modifications in continuum-containing systems. In the present work we consider a special case of coherent population trapping with a train of ultrashort pulses in a  $\Lambda$ -type energy system with two bound states and the continuum replacing the upper state. We demonstrate that if the bound states splitting is multiple of the pulse repetition rate, a medium becomes completely transparent for the optical field. Complete transparency can be realized because in this scheme incoherent ionization losses, always present in the configuration when only two fields are applied, are cancelled naturally without, for

example, a special choice of a polarization of the field. We also discuss its possible application to the problem of suppression of excited-state absorption (ESA) in laser crystals. Irreversible population loss to the continuum due to ESA of either emitted or/and pumping radiation from populated metastable levels is a severe problem preventing many optical crystals from lasing [11], especially in the ultraviolet and vacuum ultraviolet regions. Recently we proposed a method of ESA suppression at a lasing wavelength using the LICS phenomenon [12]. The idea was to apply a strong coherent laser field between the terminal state of the ESA transition for the generated radiation and some auxiliary bound state, which would result in ESA suppression leaving stimulated emission unaffected. In the present work we discuss the possibility of applying CPT with a train of pulses via the continuum to systems where only pumping radiation is absorbed from the metastable laser level, and consider a particular material,  $\text{Ti}^{3+}:\text{YAlO}_3$  crystal, where this technique can significantly increase the pumping efficiency.

Coherent population trapping in a system with three bound levels in the  $\Lambda$  configuration coupled to a laser field in the form of a pulse train was first considered by Kocharovskaya and Khanin [13] in 1986. They showed that if the lower levels splitting  $\Delta$  satisfies the condition  $\Delta = 2\pi n/T$ , where  $T$  is the period of the train,  $n$  is an integer, the medium becomes transparent for the incident radiation. Recently this idea has been verified experimentally, first in  $^{85}\text{Rb}$  vapor [14], and later in a room temperature ruby [15]. The latter experiment is especially noteworthy, being an observation of CPT in a room temperature solid and a step toward realization of the ESA suppression technique proposed in this work. Earlier, CPT was proposed as a means for stabilization of a repetition rate in a mode-locked laser by locking it to the hyperfine splitting of  $^{87}\text{Rb}$  [16].

The paper is organized in the following way. In Sec. II we theoretically consider CPT via the continuum with a train of ultrashort pulses and derive the conditions under which it takes place. In our analysis we take into account the coherence decay between the bound states since it is almost inevitable in a real experiment and therefore defines the best possible trapping case. In Sec. III we discuss a possible application of the technique to ESA suppression of pumping

\*Electronic address: [lena@jewel.tamu.edu](mailto:lena@jewel.tamu.edu)

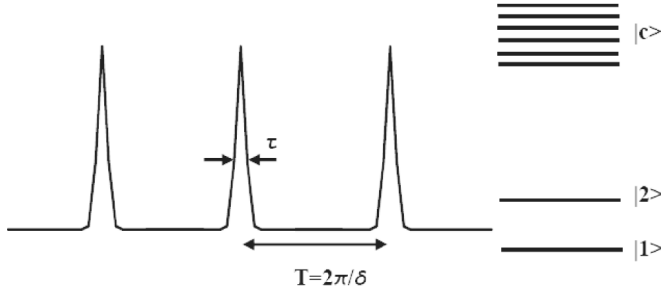


FIG. 1. Three-level  $\Lambda$  energy system with the upper level replaced by a continuum of states interacting with a train of ultrashort pulses.

radiation in laser crystals, and present results of numerical modeling of pumping with a train of pulses for the  $\text{Ti}^{3+}$ : $\text{YAIO}_3$  crystal. We finally conclude in Sec. IV.

## II. THEORY

The system we consider has two bound states  $|1\rangle$  and  $|2\rangle$  coupled to the structureless continuum  $|c\rangle$  by a train of ultrashort pulses as shown in Fig. 1. Neglecting all losses not related to ionization by the laser field allows one to describe the system by the wave function

$$|\Psi\rangle = a_1 e^{-iE_1 t/\hbar} |1\rangle + a_2 e^{-iE_2 t/\hbar} |2\rangle + \int c e^{-iE_c t/\hbar} |c\rangle dE_c,$$

where  $a_{1,2}$  and  $c$  are the probability amplitudes of states  $|1\rangle$ ,  $|2\rangle$ , and  $|c\rangle$  in the interaction representation,  $E_{1,2}$  and  $E_c$  are their energies.

The semiclassical Hamiltonian of the system can be written as  $H = H_0 + V$ , where the atomic and interaction parts are given by the expressions

$$H_0 = E_1 |1\rangle\langle 1| + E_2 |2\rangle\langle 2| + \int E_c |c\rangle\langle c| dE_c,$$

$$V = - \int \mu_{1c} \mathcal{E} |1\rangle\langle c| dE_c - \int \mu_{2c} \mathcal{E} |2\rangle\langle c| dE_c + \text{H. c.}$$

with  $\mu_{1c,2c}$  being the dipole moment matrix element of the corresponding bound state-continuum transition. The electric field component of the laser radiation is described as

$$\mathcal{E} = \frac{1}{2} \sum_n \mathcal{E}_n(t - nT) e^{-i\omega t + i\phi_n} + \text{c. c.}$$

We assume that  $\mathcal{E}_n$  are real and the pulses are identical. The duration of a single pulse  $\tau$  is much smaller than the period of the pulse train  $T$ , such that the pulses do not overlap.

Dynamic equations for the probability amplitudes in the rotating wave approximation (RWA) have the form

$$i\hbar \frac{\partial a_1}{\partial t} = -\frac{1}{2} \sum_n \mathcal{E}_n(t - nT) e^{-i\phi_n} \int \mu_{1c} c e^{-i[(E_c - E_1)/\hbar - \omega]t} dE_c, \quad (1)$$

$$i\hbar \frac{\partial a_2}{\partial t} = -\frac{1}{2} \sum_n \mathcal{E}_n(t - nT) e^{-i\phi_n} \int \mu_{2c} c e^{-i[(E_c - E_2)/\hbar - \omega]t} dE_c, \quad (2)$$

$$i\hbar \frac{\partial c}{\partial t} = -\frac{\mu_{c1}}{2} \sum_n \mathcal{E}_n(t - nT) e^{i\phi_n} e^{i[(E_c - E_1)/\hbar - \omega]t} - \frac{\mu_{c2}}{2} \sum_n \mathcal{E}_n(t - nT) e^{i\phi_n} e^{i[(E_c - E_2)/\hbar - \omega]t}. \quad (3)$$

The assumption of the structureless continuum allows one to adiabatically eliminate the continuum amplitude following the procedure outlined in Ref. [1], and reduce the system (1)–(3) to two equations for the amplitudes of the bound states

$$\begin{aligned} \frac{\partial a_1}{\partial t} &= \frac{i}{4\hbar^2} a_1 \sum_{n,m} \mathcal{E}_n \mathcal{E}_m e^{-i(\phi_n - \phi_m)} (P_1 + i\Gamma_1/2) \\ &+ \frac{i}{4\hbar^2} a_2 \sum_{n,m} \mathcal{E}_n \mathcal{E}_m e^{-i(\phi_n - \phi_m) - i[(E_2 - E_1)/\hbar]t} (\Pi_{12} + iG_{12}/2), \end{aligned} \quad (4)$$

$$\begin{aligned} \frac{\partial a_2}{\partial t} &= \frac{i}{4\hbar^2} a_2 \sum_{n,m} \mathcal{E}_n \mathcal{E}_m e^{i(\phi_n - \phi_m) + i[(E_2 - E_1)/\hbar]t} (\Pi_{21} + iG_{21}/2) \\ &+ \frac{i}{4\hbar^2} a_1 \sum_{n,m} \mathcal{E}_n \mathcal{E}_m e^{i(\phi_n - \phi_m)} (P_2 + i\Gamma_2/2). \end{aligned} \quad (5)$$

Here we introduce the following notations:

$$\begin{aligned} P_l + i\Gamma_l/2 &= \lim_{\eta \rightarrow +0} \int \frac{|\mu_{lc}|^2 dE_c}{\frac{E_c - E_l}{\hbar} - \omega - i\eta} \\ &= P \int \frac{|\mu_{lc}|^2 dE_c}{\frac{E_c - E_l}{\hbar} - \omega} + i\pi\hbar |\mu_{cl}|^2 |_{E_c = E_l + \hbar\omega}, \end{aligned} \quad (6)$$

which are the laser-induced Stark shifts and ionization rates of the bound states and

$$\begin{aligned} \Pi_{lm} + iG_{lm}/2 &= \lim_{\eta \rightarrow +0} \int \frac{\mu_{lc} \mu_{cm} dE_c}{\frac{E_c - E_m}{\hbar} - \omega - i\eta} \\ &= P \int \frac{\mu_{lc} \mu_{cm} dE_c}{\frac{E_c - E_m}{\hbar} - \omega} + i\pi\hbar \mu_{lc} \mu_{cm} |_{E_c = E_m + \hbar\omega} \end{aligned} \quad (7)$$

describe the magnitude and the phase of a two-photon coherence between bound states, giving rise to CPT, induced by Raman processes via the continuum.

Taking into account that the pulses in the train do not overlap, the system (4), (5) can be modified in the following way

$$\begin{aligned} \frac{\partial a_1}{\partial t} &= \frac{i}{4\hbar^2} a_1 \sum_n \mathcal{E}_n^2 (P_1 + i\Gamma_1/2) \\ &+ \frac{i}{4\hbar^2} a_2 \sum_n \mathcal{E}_n^2 e^{-i[(E_2-E_1)/\hbar]t} (\Pi_{12} + iG_{12}/2), \end{aligned} \quad (8)$$

$$\begin{aligned} \frac{\partial a_2}{\partial t} &= \frac{i}{4\hbar^2} a_1 \sum_n \mathcal{E}_n^2 e^{i[(E_2-E_1)/\hbar]t} (\Pi_{21} + iG_{21}/2) \\ &+ \frac{i}{4\hbar^2} a_2 \sum_n \mathcal{E}_n^2 (P_2 + i\Gamma_2/2). \end{aligned} \quad (9)$$

It is convenient to expand the intensity of the train  $\sum_n \mathcal{E}_n^2$  in a Fourier series

$$\sum_n \mathcal{E}_n^2(t - nT) = \sum_m I_m e^{-im\delta t}, \quad (10)$$

where the  $m$ th Fourier component amplitude is given by the expression  $I_m = T^{-1} \int_0^T \mathcal{E}_0^2(t) e^{i\delta m t} dt$  and  $I_{-m} = I_m^*$ . There is a relationship between the Fourier components of the intensity and the amplitude of the field  $I_m = \sum_k \mathcal{E}_k \mathcal{E}_{k-m}^*$ , where  $\sum_n \mathcal{E}_n = \sum_k \mathcal{E}_k e^{ik\delta t}$ . It shows that the  $m$ th intensity component describes a beat at the frequency  $m\delta$  produced by all frequency sidebands present in the pulse.

Turning to new variables

$$a_1 = \sum_l a_{1,l} e^{-il\delta t}, \quad (11)$$

$$a_2 = \sum_l a_{2,l} e^{i[(E_2-E_1)/\hbar - l\delta]t}, \quad (12)$$

we obtain the following equations:

$$\begin{aligned} \frac{\partial a_{1,l}}{\partial t} &= il\delta a_{1,l} + \frac{i}{4\hbar^2} \sum_k a_{1,k} I_{l-k} (P_1 + i\Gamma_1/2) \\ &+ \frac{i}{4\hbar^2} \sum_k a_{2,k} I_{l-k} (\Pi_{12} + iG_{12}/2), \end{aligned} \quad (13)$$

$$\begin{aligned} \frac{\partial a_{2,l}}{\partial t} &= -i \left( \frac{E_2 - E_1}{\hbar} - l\delta \right) a_{2,l} + \frac{i}{4\hbar^2} \sum_k a_{1,k} I_{l-k} (\Pi_{21} + iG_{21}/2) \\ &+ \frac{i}{4\hbar^2} \sum_k a_{2,k} I_{l-k} (P_2 + i\Gamma_2/2). \end{aligned} \quad (14)$$

To simplify further analysis we assume that  $\delta \gg |I_0(P_1 + i\Gamma_1/2)|/4\hbar^2$ ,  $\delta \gg |I_0(P_2 + i\Gamma_2/2)|/4\hbar^2$  [where  $l_0$  is the Fourier component resonant to the two-photon Raman transition  $|1\rangle \leftrightarrow |2\rangle$ , so that the condition  $|(E_2 - E_1)/\hbar - l_0\delta| \ll \delta$  is satisfied]. It is clear from Eqs. (13), (14) that in this case only  $a_{1,0}$  and  $a_{2,l_0}$  are non-negligible. Other terms will be correspondingly, smaller by the factors  $|I_0(P_1 + i\Gamma_1/2)|/4\hbar^2\delta$  and  $|I_0(P_2 + i\Gamma_2/2)|/4\hbar^2\delta$ . This assumption allows one to take into account only one beat note with the frequency  $l_0\delta$ , resonant with the Raman transition, all other beat notes will be far from the resonance, since  $\delta$  is much larger than the Raman transition width.

With only  $a_{1,0}$  and  $a_{2,l_0}$  left, the system (13), (14) is reduced to the set

$$\frac{\partial a_{1,0}}{\partial t} = \frac{i}{4\hbar^2} I_0 (P_1 + i\Gamma_1/2) a_{1,0} + \frac{i}{4\hbar^2} I_{-l_0} a_{2,l_0} (\Pi_{12} + iG_{12}/2), \quad (15)$$

$$\begin{aligned} \frac{\partial a_{2,l_0}}{\partial t} &= \frac{i}{4\hbar^2} I_{l_0} (\Pi_{21} + iG_{21}/2) a_{1,0} + \left[ -i \left( \frac{E_2 - E_1}{\hbar} - l_0\delta \right) \right. \\ &\left. + \frac{i}{4\hbar^2} I_0 (P_2 + i\Gamma_2/2) \right] a_{2,l_0}. \end{aligned} \quad (16)$$

To simplify the equations we denote

$$I_0 \Gamma_{1,2} / 8\hbar^2 = G_{1,2},$$

$$I_0 P_{1,2} / 4\hbar^2 = \delta E_{1,2},$$

$$G_{21} I_{l_0} / 8\hbar^2 = G,$$

$$\Delta_{l_0} = \frac{E_2 - E_1}{\hbar} - l_0\delta,$$

and introduce the Fano asymmetry parameter  $q$  (assumed real) as

$$q = 2\Pi_{12}/G_{12} = 2\Pi_{21}/G_{21}.$$

Finally let us make a substitution following Ref. [18]:

$$a_{1,0}, a_{2,l_0} = \alpha_{1,2} \exp\left(i \int_0^t (\delta E_1 - qG_1) dt\right)$$

to obtain the following set of equations for the new variables:

$$\frac{\partial \alpha_1}{\partial t} = iG_1(q+i)\alpha_1 + iG^*(q+i)\alpha_2, \quad (17)$$

$$\begin{aligned} \frac{\partial \alpha_2}{\partial t} &= iG(q+i)\alpha_1 + [i(\delta E_2 - \delta E_1) - i\Delta_{l_0} + iG_2(q+i) \\ &+ iq(G_1 - G_2)]\alpha_2. \end{aligned} \quad (18)$$

It is customary to denote the term in figure brackets in Eq. (18) as  $i\Delta + iG_2(q+i)$ , where  $\Delta = \delta E_2 - \delta E_1 - \Delta_{l_0} + q(G_1 - G_2)$ . The system (17), (18) can then be written in the following matrix form:

$$\frac{\partial}{\partial t} \begin{pmatrix} \alpha_1 \\ \alpha_2 \end{pmatrix} = i \begin{pmatrix} G_1(q+i) & G^*(q+i) \\ G(q+i) & \Delta + G_2(q+i) \end{pmatrix} \begin{pmatrix} \alpha_1 \\ \alpha_2 \end{pmatrix}. \quad (19)$$

The eigenvalues of the Hamiltonian in Eq. (19) define the evolution of system, the corresponding characteristic equation

$$\begin{aligned} \lambda^2 - \lambda[i\Delta + i(G_1 + G_2)(q+i)] - \Delta G_1(q+i) \\ - (G_1 G_2 - |G|^2)(q+i)^2 = 0 \end{aligned} \quad (20)$$

has the eigenvalues

$$\lambda_{1,2} = \frac{i\Delta + i(G_1 + G_2)(q + i)}{2} \pm \sqrt{\left(\frac{i\Delta + i(G_1 + G_2)(q + i)}{2}\right)^2 + \Delta G_1(q + i) + (G_1 G_2 - |G|^2)(q + i)^2}. \quad (21)$$

Assuming that the single pulse in the train is sufficiently short such that its spectral width significantly exceeds the splitting  $(E_2 - E_1)/\hbar$  between the bound states, we would have  $|I_0| \approx |I_{l_0}|$ . The latter condition means that the Fourier components of the amplitude of the pulse satisfy the condition  $|\varepsilon_m| \approx |\varepsilon_{m+l_0}|$ . It results in  $G_1 G_2 - |G|^2 \approx 0$ . Then at two-photon resonance  $\Delta = 0$  the eigenvalues are

$$\lambda_1 = i(G_1 + G_2)(q + i), \quad (22)$$

$$\lambda_2 = 0. \quad (23)$$

The zero eigenvalue is a signature of coherent population trapping. It means that if the system is initially in the “dark” superposition of bound states  $|\Psi\rangle_d = (\sqrt{G_2}|1\rangle - \sqrt{G_1}|2\rangle)/\sqrt{G_1 + G_2}$ , it will not interact with the train. In a general case, when initially some fraction of the population is in the “dark” and the rest is in the orthogonal “bright” state  $|\Psi\rangle_b = (\sqrt{G_1}|1\rangle + \sqrt{G_2}|2\rangle)/\sqrt{G_1 + G_2}$ , the train will transfer the “bright” state population to the continuum with the rate  $-\text{Re } \lambda_1 = G_1 + G_2$  leaving the “dark” state unaffected. It is worth noting that close to the two-photon resonance the CPT eigenvalue is

$$\lambda_2 \approx \frac{i\Delta G_1}{G_1 + G_2} - \frac{\Delta^2(1 + iq)|G|^2}{(G_1 + G_2)^3(q^2 + 1)},$$

resulting in the width of the CPT resonance in absorption

$$\Delta_{CPT} = \sqrt{\frac{(G_1 + G_2)^3(q^2 + 1)}{|G|^2 t}}, \quad (24)$$

which is proportional to the square root of the ratio of the ionization rate to time. This is a general rule for the CPT resonance in an open system, where population irreversibly decays out of the system [17]. Another important remark is that in the case considered here compared to the typically considered one with only two fields [18], pump and probe, it is possible to have complete CPT at  $\Delta = 0$ , while in the latter one complete transparency is not possible. The reason is two-fold. First, in our case it is easy to satisfy the condition  $\Delta = 0$ , since  $\Delta$  is a real function, while in the case with two fields the two-photon resonance detuning is a complex function

$$\Delta = \delta E_2 - \delta E_1 - D^{ab} + q(G_1^a - G_2^b) + i(G_2^a - G_1^b),$$

where  $D^{ab} = \frac{E_2 - E_1}{\hbar} - (\omega_a - \omega_b)$ ,  $G_{1,2}^a = |E_a|^2 \Gamma_{1,2}^a / 8\hbar^2$ ,  $G_{1,2}^b = |E_b|^2 \Gamma_{1,2}^b / 8\hbar^2$  for the two fields with frequencies  $\omega_{a,b}$  and amplitudes  $E_{a,b}$ . It is clear that  $\Delta$  can be set exactly to zero only if  $G_2^a = G_1^b$ . Even if this requirement is met, CPT is not complete because each field interacts with both bound states, which results in incoherent ionization losses. In the case with the train of pulses each frequency component of the field is

matched by another component detuned by the two-photon resonance frequency. All components thus form a series of two-photon resonant  $\Lambda$  systems, preventing any incoherent losses.

It is worthwhile, based on the previous discussion, to make a remark about techniques utilized for population transfer and coherence creation in molecules, for example superposition states via stimulated Raman adiabatic passage, which use ultrashort (fs duration) pulses. Using such broadband pulses with pulse bandwidths approaching frequencies of vibrational transitions can degrade the efficiency of the process. In that case both the pump and the Stokes fields interact with both optical transitions in the  $\Lambda$  system. It means that neither the initial nor the final state is a “dark” state and as a result only partial population transfer is possible. The configuration considered in the present work is different. Pumping with a train of laser pulses allows one to consider the interaction of pulses with the  $\Lambda$  energy-level system as a steady-state process. Namely, the laser radiation can be considered as a multifrequency electromagnetic field with the separation between frequency components determined by the pulse repetition rate. When the separation is much larger than the width of the transition between lower levels in the  $\Lambda$  system, and the pulses bandwidth significantly exceeds the frequency of the transition, the “dark” state is the same for all pairs of frequency components which are close to a two-photon resonance with the lower levels. The coupling of the “dark” state to the “bright” one originates from a finite bandwidth of the pulses resulting in different amplitudes of the frequency components. In turn, for the frequency components with different amplitudes the corresponding “dark” state is slightly different. So the “dark” state starts interacting with these frequency components, which is equivalent to the coupling between the “dark” and “bright” states. If the pulses bandwidth significantly exceeds the lower level separation, this coupling is weak.

Let us now consider a more realistic case when coherence relaxation between bound states  $|1\rangle$  and  $|2\rangle$  is present and find how the dynamics of the system is modified. To do this we will turn to the density matrix description and include the relaxation phenomenologically. Namely, we introduce diagonal  $\rho_{11} = \alpha_1 \alpha_1^*$ ,  $\rho_{22} = \alpha_2 \alpha_2^*$  and off-diagonal  $\sigma_{21} = \alpha_2 \alpha_1^*$  density matrix elements, describing populations and bound-state coherence, respectively. From Eq. (19) the time evolution of the density matrix elements is given by

$$\frac{d\rho_{11}}{dt} = -2G_1\rho_{11} + iG^*(q + i)\sigma_{21} - iG(q - i)\sigma_{21}^*, \quad (25)$$

$$\frac{d\rho_{22}}{dt} = -2G_2\rho_{22} - iG^*(q - i)\sigma_{21} + iG(q + i)\sigma_{21}^*, \quad (26)$$

$$\begin{aligned} \frac{d\sigma_{21}}{dt} = & -\{i[\Delta + G_2(q+i) - G_1(q-i)] + \gamma_{21}\}\sigma_{21} \\ & + iG(q+i)\rho_{11} - iG(q-i)\rho_{22}, \end{aligned} \quad (27)$$

where the coherence decay term  $\gamma_{21}$  describing pure dephasing processes is included.

It is more convenient to turn to the real and imaginary parts of the coherence

$$S^+ = \frac{\sigma_{21} + \sigma_{21}^*}{2}, \quad S^- = \frac{\sigma_{21} - \sigma_{21}^*}{2i}. \quad (28)$$

The system (25)–(27) now is written in the form (assuming  $G$  real)

$$\frac{d\rho_{11}}{dt} = -2G_1\rho_{11} - 2GqS^- - 2GS^+, \quad (29)$$

$$\frac{d\rho_{22}}{dt} = -2G_2\rho_{22} + 2GqS^- - 2GS^+, \quad (30)$$

$$\begin{aligned} \frac{dS^+}{dt} = & -(G_1 + G_2 + \gamma_{21})S^+ - [\Delta + q(G_2 - G_1)]S^- \\ & - G(\rho_{11} + \rho_{22}), \end{aligned} \quad (31)$$

$$\begin{aligned} \frac{dS^-}{dt} = & -(G_1 + G_2 + \gamma_{21})S^- + [\Delta + q(G_2 - G_1)]S^+ \\ & + Gq(\rho_{11} - \rho_{22}). \end{aligned} \quad (32)$$

The eigenvalues of this system can be found from the characteristic equation

$$\begin{aligned} & [\lambda^2 + 2\lambda(G_1 + G_2 + \gamma_{21})][\lambda^2 + 2\lambda(G_1 + G_2)] \\ & + 4|G|^2[\lambda^2 + 2\lambda(G_1 + G_2 + \gamma_{21})] \\ & + [\lambda^2 + 2\lambda(G_1 + G_2)](G_1 + G_2 + \gamma_{21})^2 \\ & + [\lambda^2 + \lambda(2G_1 + 2G_2 + \gamma_{21})]4G^2(q^2 - 1) \\ & + [\lambda^2 + 2\lambda(G_1 + G_2)][\Delta + q(G_2 - G_1)]^2 \\ & + 4G^2\gamma_{21}(2G_1 + 2G_2 + \gamma_{21}) + 4G^2\Delta^2 = 0, \end{aligned} \quad (33)$$

where we used  $G_1G_2 = G^2$ .

To find the eigenvalue corresponding to CPT we assume that the dephasing is weak:  $\gamma_{21} \ll G_1, G_2$ . This assumption is well justified since if  $\gamma_{21} \gg G_1, G_2$  there is no CPT and no ionization suppression is possible. We also assume that this eigenvalue is  $\sim \gamma_{21}$ , i.e., small. Equation (33) then simplifies as

$$\begin{aligned} \lambda^2 + \frac{1}{2}\lambda\left((q^2 + 1)(G_1 + G_2) + \frac{\Delta^2 + 2\Delta q(G_2 - G_1)}{G_1 + G_2}\right) \\ + \frac{2G^2\gamma_{32}}{G_1 + G_2} + \frac{G^2\Delta^2}{(G_1 + G_2)^2} = 0. \end{aligned} \quad (34)$$

For small detunings  $\Delta \ll G_1, G_2$  the CPT eigenvalue is given by

$$\begin{aligned} \lambda_{\text{CPT}} = & -\frac{q^2 + 1}{4}(G_1 + G_2) \\ & + \sqrt{\left(\frac{q^2 + 1}{4}(G_1 + G_2)\right)^2 - \frac{2G^2\gamma_{21}}{G_1 + G_2} - \frac{G^2\Delta^2}{(G_1 + G_2)^2}} \end{aligned} \quad (35)$$

or

$$\lambda_{\text{CPT}} = -\frac{4G^2\gamma_{21}}{(q^2 + 1)(G_1 + G_2)^2} - \frac{2G^2\Delta^2}{(q^2 + 1)(G_1 + G_2)^3}. \quad (36)$$

At the exact two-photon resonance the rate of population decay to the continuum is thus

$$\lambda_{\text{CPT}} = -\frac{4G^2\gamma_{21}}{(q^2 + 1)(G_1 + G_2)^2} \approx -\gamma_{21}, \quad (37)$$

if the ionization rates are of the same magnitude. This decay rate has to be compared with the one when there is no coherence (for example, in the limit of very fast decoherence  $\gamma_{21} \gg G_1, G_2$ ). The slowest decay process is described in this case by the roots  $\lambda_{1,2} \approx -2G_{1,2}$ , so the ionization is reduced by the factor  $G_{1(2)}/\gamma_{21}$  if CPT is induced. As follows from Eq. (36) the CPT resonance width at the moment  $t$  is the same as in the  $\gamma_{21} = 0$  limit [see Eq. (24)]

$$\Delta_{\text{CPT}} = \sqrt{\frac{(G_1 + G_2)^3(q^2 + 1)}{2G^2t}}. \quad (38)$$

### III. APPLICATION OF CPT WITH A TRAIN OF PULSES TO SUPPRESSION OF EXCITED-STATE ABSORPTION OF PUMPING RADIATION IN OPTICAL CRYSTALS

In this section we apply the results obtained in the previous section to a particular problem of suppression of excited-state absorption in optical crystals. As an example we consider a  $\text{Ti}^{3+}:\text{YAlO}_3$  material. This crystal, very close in its characteristics to the famous  $\text{Ti}^{3+}:\text{Al}_2\text{O}_3$  laser crystal, has its fluorescence band shifted to shorter wavelengths, lying in the range 550–750 nm. Its short wavelength part covers the important yellow-orange spectral region, which is of increasing interest for a number of applications in laser medical research due to high absorption of hemoglobin in this range, navigation and astrophysics in, for example, Laser Guide Star Adaptive Optics. Nowadays, this region is mostly covered by dye lasers and OPO's, there are few fixed-wavelength solid-state lasers operating in this range: frequency-doubled Cr:forsterite and Nd: $\text{Sr}_5(\text{PO}_4)_3\text{F}$  (Nd:SFAP) lasers, Nd:YVO<sub>4</sub> laser having its 1.3 and 1.06  $\mu\text{m}$  outputs summed, and Raman-shifted Nd:YAG second harmonic lasers [19]. The only tunable crystalline laser operating in the range 540–620 nm is a  $\text{Al}_2\text{O}_3$  color center laser [20], but color center lasers are known to be photounstable and thermounstable. It would therefore be of significant technological importance to have a compact tunable laser based on transition metal or rare earth ion doped crystals covering this part of the spectrum.

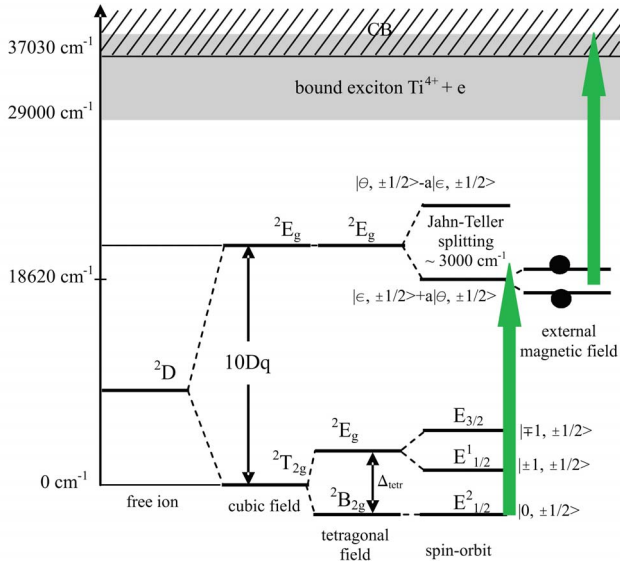


FIG. 2. (Color online) Energy-level diagram of  $\text{Ti}^{3+}:\text{YAlO}_3$  including crystal field, spin-orbit interactions, Jahn-Teller effect, and the effect of an external magnetic field. Pumping with the second harmonic of Nd:YAG laser (532 nm) and excited-state absorption of the pump are schematically illustrated.

Having such promising characteristics,  $\text{Ti}^{3+}:\text{YAlO}_3$  has not turned into a laser material because of very inefficient pumping (0.044%, as was reported in Ref. [21]). The main reason is excited-state absorption of pumping radiation from a metastable laser transition level that sets at wavelengths shorter than 550 nm. It means that, luckily, emission is not affected by ESA, only pumping radiation is absorbed. The absorption goes into a charge-transfer band, related to bound exciton  $\text{Ti}^{4+}+e$  formation, overlapping the conduction band of the crystal. The energy level scheme of the  $\text{Ti}^{3+}$  ion in the  $\text{YAlO}_3$  host is shown in Fig. 2 [22–27]. In an octahedral crystalline field produced by six surrounding oxygen ions a degenerate  $3d^1$  state of a free ion splits into  ${}^2E_g$  and  ${}^2T_{2g}$  states, which are further split by tetragonal crystal field distortions, spin-orbit and Jahn-Teller interactions. Final states are degenerate Kramers doublets, which is a general rule for ions with odd number of electrons in an unfilled shell. The excited state Kramers doublets, having an effective spin 1/2, can be further Zeeman split in an external magnetic field. When pumped with a train of pulses, excited-state absorption of population stored in the Zeeman sublevels of the metastable laser level will be suppressed if the Zeeman splitting is a multiple of the repetition rate. The same reasoning applies also to  $\text{V}^{4+}$  (isoelectronic with  $\text{Ti}^{3+}$ ) doped  $\text{YAlO}_3$  crystal, having similar to  $\text{Ti}^{3+}:\text{YAlO}_3$  characteristics [28,29].

In order to make more clear how the technique discussed in the theoretical part can be applied to suppression of ESA of pumping radiation in  $\text{Ti}^{3+}:\text{YAlO}_3$  we use a simplified energy level structure of the latter shown in Fig. 3. In this figure  $|1\rangle$  denotes the ground state  ${}^2E_{1/2}$  of the ion;  $|2\rangle$  and  $|3\rangle$  are the Zeeman sublevels of the metastable excited state,  $\Delta_{32}$  is the corresponding Zeeman splitting;  $|4\rangle$  is some intermediate state in the excited state phonon sideband used for pumping population to the metastable state;  $|5\rangle$  is some state

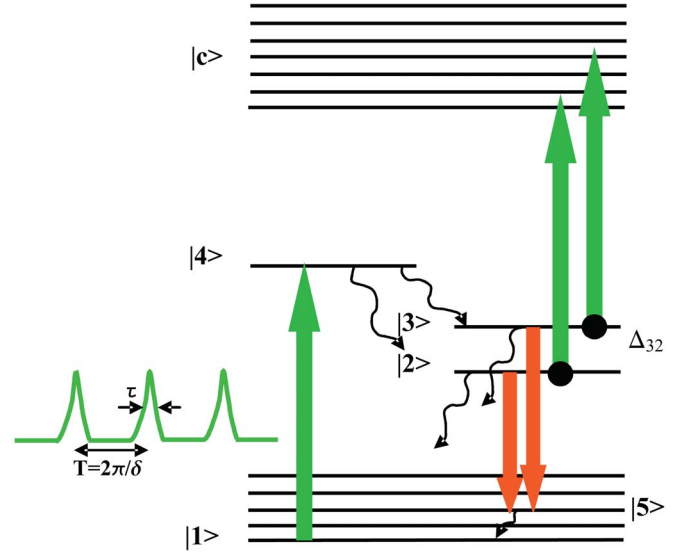


FIG. 3. (Color online) Five-level plus continuum energy system used to model pumping of  $\text{Ti}^{3+}:\text{YAlO}_3$  with a train of ultrashort pulses.

in the phonon sideband of the ground state, the terminal state of the emission transition;  $|c\rangle$  is the continuum used to model the charge transfer (bound exciton  $\text{Ti}^{4+}+e$ ) and the conduction bands of the crystal. Thus excited state absorption of pumping radiation from the Zeeman sublevels  $|2\rangle$  and  $|3\rangle$  of the metastable excited state to the continuum, shown in Fig. 3 by green arrows, is to be suppressed. A pumping pulse (in the numerical model we assume pumping with a second harmonic of a Nd:YAG laser,  $\lambda=532$  nm) excites the  $\text{Ti}^{3+}$  ion from the ground state to some excited phonon state of the metastable level, from which it rapidly (in picosecond time) decays to the pure electronic state. Due to excited-state absorption the pumping radiation transfers population from the metastable electronic state into the charge-transfer band. The cross section of this transfer process is about 50 times higher than the ground-state absorption one [30], thus making pumping very inefficient. To suppress excited-state absorption pumping with a train of ultrashort pulses can be applied, making use of the coherent population trapping effect.

We used the density matrix approach to model the dynamics of the pumping process. Taking into account fast nonradiative population decay from the intermediate phonon states  $|4\rangle$  and  $|5\rangle$  to the pure electronic metastable states  $|2\rangle$  and  $|3\rangle$  and the ground state  $|1\rangle$ , respectively, allowing one to set all coherences except  $\sigma_{41}$  and  $\sigma_{32}$  to zero, the system can be described by the following set of equations:

$$\sigma_{41} = \frac{i \sum_n \Omega_n^{41} (\rho_{11} - \rho_{44})}{\gamma_{41} + \frac{\sum_n \mathcal{E}_n^2(t-nT)}{8\hbar^2} \Gamma_4}, \quad (39)$$

$$\begin{aligned} \frac{\partial \sigma_{32}}{\partial t} = & - \left( i\Delta_{32} + \gamma_{32} + \frac{\sum_n \mathcal{E}_n^2(t-nT)}{8\hbar^2} (\Gamma_2 + \Gamma_3) \right) \sigma_{32} \\ & + i\rho_{22} \frac{\sum_n \mathcal{E}_n^2(t-nT)}{8\hbar^2} G_{32}(i+q_{32}) \\ & - i\rho_{33} \frac{\sum_n \mathcal{E}_n^2(t-nT)}{8\hbar^2} G_{23}(i+q_{23}), \end{aligned} \quad (40)$$

$$\begin{aligned} \frac{\partial \rho_{11}}{\partial t} = & i \sum_n (\Omega_n^{41})^* \sigma_{41} - i \sum_n \Omega_n^{41} \sigma_{41}^* + W_{21}\rho_{22} \\ & + W_{31}\rho_{33} + W_{51}\rho_{55}, \end{aligned} \quad (41)$$

$$\begin{aligned} \frac{\partial \rho_{22}}{\partial t} = & - \left( \frac{\sum_n \mathcal{E}_n^2(t-nT)}{4\hbar^2} \Gamma_2 + W_{23} + W_{21} + W_{25} \right) \rho_{22} + W_{42}\rho_{44} \\ & + W_{32}\rho_{33} + i\sigma_{32} \frac{\sum_n \mathcal{E}_n^2(t-nT)}{8\hbar^2} G_{23}(q_{23}+i) \\ & - i\sigma_{32}^* \frac{\sum_n \mathcal{E}_n^2(t-nT)}{8\hbar^2} G_{22}(q_{23}-i), \end{aligned} \quad (42)$$

$$\begin{aligned} \frac{\partial \rho_{33}}{\partial t} = & - \left( \frac{\sum_n \mathcal{E}_n^2(t-nT)}{4\hbar^2} \Gamma_3 + W_{32} + W_{31} + W_{35} \right) \rho_{33} + W_{43}\rho_{44} \\ & + W_{23}\rho_{22} + i\sigma_{32}^* \frac{\sum_n \mathcal{E}_n^2(t-nT)}{8\hbar^2} G_{32}(q_{32}+i) \\ & - i\sigma_{32} \frac{\sum_n \mathcal{E}_n^2(t-nT)}{8\hbar^2} G_{32}(q_{32}-i), \end{aligned} \quad (43)$$

$$\rho_{44} = \frac{i \sum_n \Omega_n^{41} \sigma_{41}^* - i \sum_n (\Omega_n^{41})^* \sigma_{41}}{\frac{\sum_n \mathcal{E}_n^2(t-nT)}{4\hbar^2} \Gamma_4 + W_{42} + W_{43}}, \quad (44)$$

$$\rho_{55} = \frac{W_{35}\rho_{33} + W_{25}\rho_{22}}{W_{51}}, \quad (45)$$

$$\rho_c = 1 - \rho_{11} - \rho_{22} - \rho_{33} - \rho_{44} - \rho_{55}, \quad (46)$$

where  $\Delta_{32} = (E_3 - E_2)/\hbar + \sum_n \mathcal{E}_n^2(t-nT)(P_2 - P_3)/4\hbar^2$  is the dynamic-Stark modified Zeeman splitting of the upper state;  $\Gamma_i$ ,  $P_i$ ,  $G_{32(23)}$ , and  $q_{32(23)}$  defined as in Eqs. (6), (7);  $\gamma_{ij}$  and  $W_{ij}$  are the corresponding coherence and population decay rates and  $\Omega_n^{41} = \mu_{41}\mathcal{E}_n/2\hbar$  is the pumping field Rabi frequency.

The train was modeled as a sequence of Gaussian pulses of the form  $\mathcal{E}_n = \mathcal{E}^{\max} \exp[-(t-nT - \tau/2)^2/2(\tau/4\sqrt{2})^2]$  (with the FWHM of a pulse given by  $\tau\sqrt{\ln 2/2}$ ) for  $nT < t < nT + \tau$ , and zero otherwise. The number of pulses in the train was varied in order to verify the predictions of the previous section and to find the optimal pumping conditions. The dynamics of the system critically depends on the Zeeman decoherence rate  $\gamma_{32}$ , since CPT is efficient only for  $t \leq \gamma_{32}^{-1}$ . For  $\text{Ti}^{3+}:\text{YAlO}_3$  this rate is not known, so we choose its value based on the following grounds. At room temperature spin transitions of transition metal ions in crystals are broadened by spin-lattice relaxation due to interaction with phonons. This broadening includes direct, Raman, and Orbach phonon processes, the latter two mediated by higher energy electronic states [24]. The temperature dependence of the three processes is different, at room temperature the direct process rate is proportional to  $T$ , the Raman one is proportional to  $T^2$ , for the Orbach relaxation the broadening is governed by a factor  $\exp(-\Delta E/kT)$ , where  $\Delta E$  is the energy separating the closest higher energy electronic state and the state of interest. The Orbach process dominates at room temperature if the closest excited electronic state can be reached by phonons. Typical phonon energies in crystals are several hundred  $\text{cm}^{-1}$ . In  $\text{Ti}^{3+}:\text{YAlO}_3$  the Jahn-Teller interaction splits the excited electronic state for about  $3000 \text{ cm}^{-1}$ , which would result in small Orbach broadening, making the Raman process the dominant one (direct phonon transitions between levels of a Kramers doublet are forbidden, becoming weakly allowed only if the doublet is split in a magnetic field [25]). This situation closely resembles the case of ruby, analyzed in Ref. [15], where CPT with the train of ultrashort pulses was observed in ground state Zeeman sublevels at room temperature and the width of the detected resonances was  $\sim 50 \text{ MHz}$ . So while  $\gamma_{32}$  for the Zeeman transitions in the excited state has yet to be measured in  $\text{Ti}:\text{YAlO}_3$ , comparison with ruby suggests that  $\gamma_{32}$  is expected to be of the order of tens MHz. In our numerical model we take  $\gamma_{32} = 50 \text{ MHz}$ . In the calculations we used the parameters of  $\text{Ti}^{3+}:\text{YAlO}_3$ , known from literature: ESA cross section for  $532 \text{ nm}$  pumping  $\sigma_{\text{ESA}} \sim 10^{-18} \text{ cm}^2$  [26], where  $\sigma_{\text{ESA}} = \pi\omega\Gamma_{\text{ion}}/\hbar c n(\omega)$  gives the ionization rates (we assumed for simplicity  $\Gamma_{\text{ion}} = \Gamma_2 = \Gamma_3 = \Gamma_4$ ), the ground-state absorption cross section  $\sigma_{\text{GSA}} \approx 2 \times 10^{-20} \text{ cm}^2$  [30], where  $\sigma_{\text{GSA}} = 2\pi\omega|\mu_{41}|^2/\gamma_{41}c\hbar n(\omega)$  allows one to calculate the pumping rate  $|\Omega_{41}^n|^2/\gamma_{41}$ ,  $G_{23} = G_{32} = \sqrt{\Gamma_2\Gamma_3}$ ,  $q_{32} = q_{23} = q$ ,  $W_{21}^{-1} = W_{31}^{-1} = W_{25}^{-1} = W_{35}^{-1} = 11.4 \mu\text{s}$  [30],  $W_{42}^{-1} = W_{43}^{-1} = W_{51}^{-1} \sim 1 \text{ ps}$ , and  $W_{32} = W_{23} = \gamma_{32}$ .

Population of the metastable Zeeman sublevel  $\rho_{22}$  and of the continuum  $\rho_c$  as a function of the splitting between the sublevels at a fixed pulse repetition rate is shown in Fig. 4. As can be seen, when the Zeeman splitting is multiple of the repetition rate  $\Delta_{32} = l\delta$ , population transfer to the continuum is slowed down and the population stored in the Zeeman sublevels is increased. The increase is  $\geq 10$  times compared to the nonresonant situation (for example, for  $\Delta_{32} = 0.5\delta$ ). It is worth noting that there is efficient CPT at zero Zeeman splitting (ground-state Hanle effect), similar to the one observed in ruby at ground-state spin sublevels [15], meaning that it is possible to efficiently pump this system even in zero magnetic field. An additional advantage of nonzero magnetic

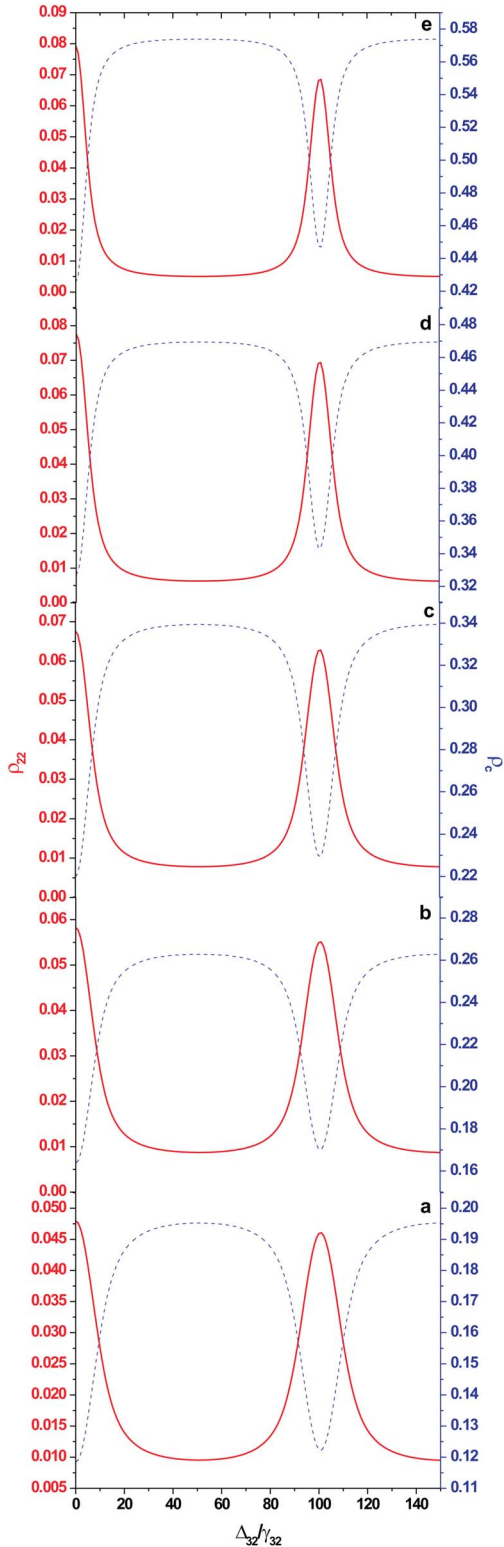


FIG. 4. (Color online) Population of the metastable Zeeman sublevel (solid line)  $\rho_{22}$  and the continuum  $\rho_c$  (dashed line) for different number of pulses, corresponding to different total pumping time. Repetition rate  $\delta=500$  MHz, pulse duration  $\tau=30$  ps, peak intensity  $I^{\max}=7$  GW/cm<sup>2</sup>;  $q=0$  meaning  $\rho_{22}=\rho_{33}$ , therefore only  $\rho_{22}$  is shown; number of pulses in the train: (a)  $N=11$ , (b)  $N=15$ , (c)  $N=20$ , (d)  $N=30$ , (e)  $N=40$ .

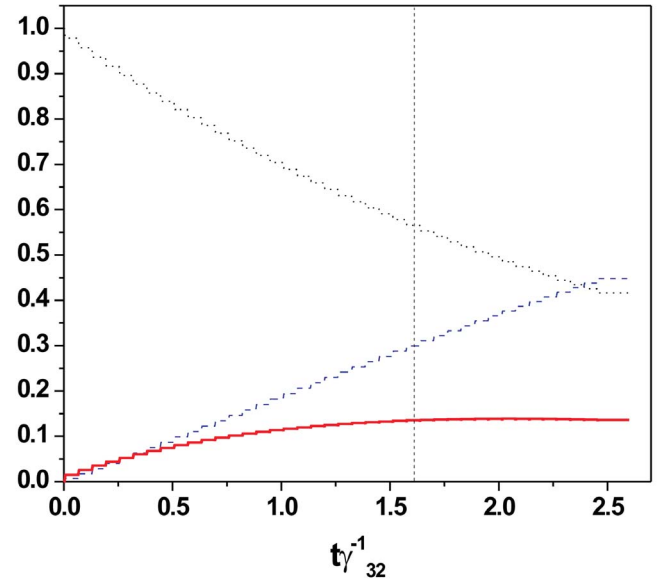


FIG. 5. (Color online) Total population in the metastable Zeeman sublevels  $\rho_{22}+\rho_{33}$  (solid line), ground state (dotted line), and in the continuum (dashed line) in the case of pumping with a train of ultrashort pulses. Pulse train parameters are the same as in Fig. 4, total number of pulses in the train  $N=40$ ,  $q=0$ . Dashed vertical line denotes the moment the threshold inversion  $(\rho_{22}+\rho_{33})/\rho_{11}=0.24$  is reached, the required number of pulses  $N\approx 30$ .

fields, though, is that the Zeeman decoherence rate can be significantly reduced if a magnetic field is applied due to suppression of dipole-dipole interaction between <sup>27</sup>Al ions of the host, inducing a fluctuating magnetic field at a Ti<sup>3+</sup> site. It would allow one to use longer and less energetic trains to obtain threshold inversion.

The threshold inversion  $(\rho_{22}+\rho_{33})/\rho_{11}=\sigma_{\text{res abs}}/\sigma_{\text{em}}=0.24$ , necessary to overcome residual absorption in the emission range ( $\sigma_{\text{res abs}}\approx 8.8\times 10^{-21}$  cm<sup>2</sup>,  $\sigma_{\text{em}}\approx 3.7\times 10^{-20}$  cm<sup>2</sup> at  $\lambda_{\text{em}}=600$  nm), is reached at peak pumping intensity of  $I^{\max}=7$  GW/cm<sup>2</sup>, when pumped with a train consisting of about 30 pulses of 30 ps duration, as shown in Fig. 5. Pumping is most efficient for trains with duration not significantly exceeding  $\gamma_{32}^{-1}$ , as was already discussed in the previous section. For longer trains population of the metastable state still grows but slower, and most of the population is transferred to the continuum since CPT is less and less efficient. At times less than  $\gamma_{32}^{-1}$  CPT is close to the ideal one, and the dynamics is close to the one expected in an open system. Namely, the Zeeman sublevels population is distributed between the “bright” and “dark” states, the “bright” state population is completely transferred to the continuum after the action of the pulse train. In our case the “bright” and “dark” states are populated equally for  $q_{23}=q_{32}=0$  and by the end of the train the population in the continuum is almost equal to the population in the metastable state, as is shown in Fig. 6. The resonances become narrower with time, again in accord with the previous section discussion.

In Fig. 7 the effect of  $q$  is analyzed. As was discussed in Ref. [3]  $|q|>1$  is detrimental for ionization suppression, since only two laser fields were used in that work, and one of them

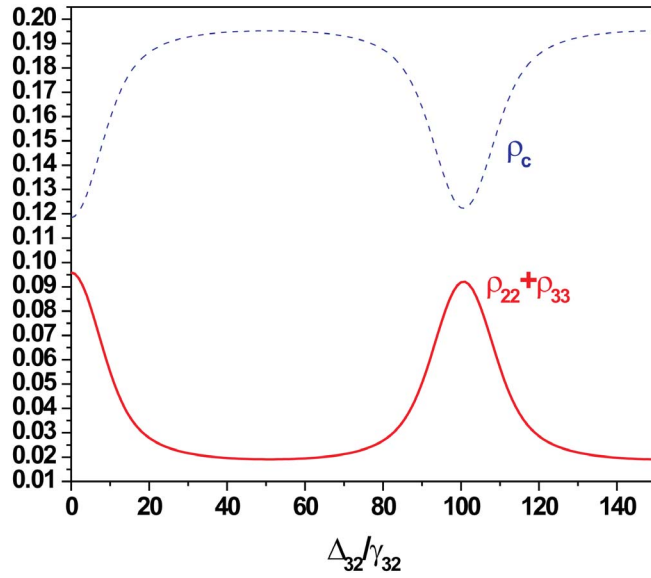


FIG. 6. (Color online) Total population in the metastable Zeeman sublevels (solid line) and in the continuum (dashed line) for pumping time  $\leq \gamma_{32}^{-1}$  when CPT is most efficient. Population in the continuum, pumped out from the “bright” state, is almost equal to the population in Zeeman sublevels, the “dark” state. Pulse train parameters are the same as in Fig. 4, number of pulses in the train  $N=11$ .

coupled both bound states to the continuum leading to incoherent ionization losses. For  $|q| \gg 1$  Raman transitions via the continuum dominate over direct transitions and it opens the way to multiphoton incoherent ionization. In our case there are no incoherent ionization channels and the influence of  $q$  is not dramatic, as can be seen from Fig. 7. It breaks the symmetry between the states  $|2\rangle$  and  $|3\rangle$  and makes the population profiles asymmetric, but the total metastable state population is the same as in the case  $q=0$  for the same pumping intensity. As can be seen from Fig. 7, nonzero  $q$  increases the width of the transparency window in  $\rho_c$ , according to Eq. (24).

In the above theory we assumed transitions from the spin Zeeman sublevels to the continuum to be of equal strength for simplicity. In reality it would require sufficient spin-orbit mixing in the continuum, allowing to couple the spin sublevels via the same continuum states. Spin-orbit interaction in the continuum was found crucial in a similar configuration, where two bound states having  $\pm 1/2$  spin components were coupled to the continuum, and utilized for production of spin-polarized photoelectrons via LICS [32]. Theoretical calculations for Rb and Cs performed in that study showed strong spin-orbit coupling for both of these atoms, for Cs being stronger than for Rb. Strong spin-orbit coupling in the continuum was experimentally observed in xenon, where LICS was used to control ionization products into two spin-orbit  $^2P_{1/2}$  and  $^2P_{3/2}$  continua of  $\text{Xe}^+$  [4,31]. Significant conduction band spin-orbit splitting was also measured in semiconductors (in the range of 0.1–0.4 eV with several eV bandgaps [33,34]). Based on these data, it is reasonable to assume that for  $\text{Ti}^{3+}:\text{YAlO}_3$  the spin-orbit interaction in the continuum is non-negligible either. Another issue not ad-

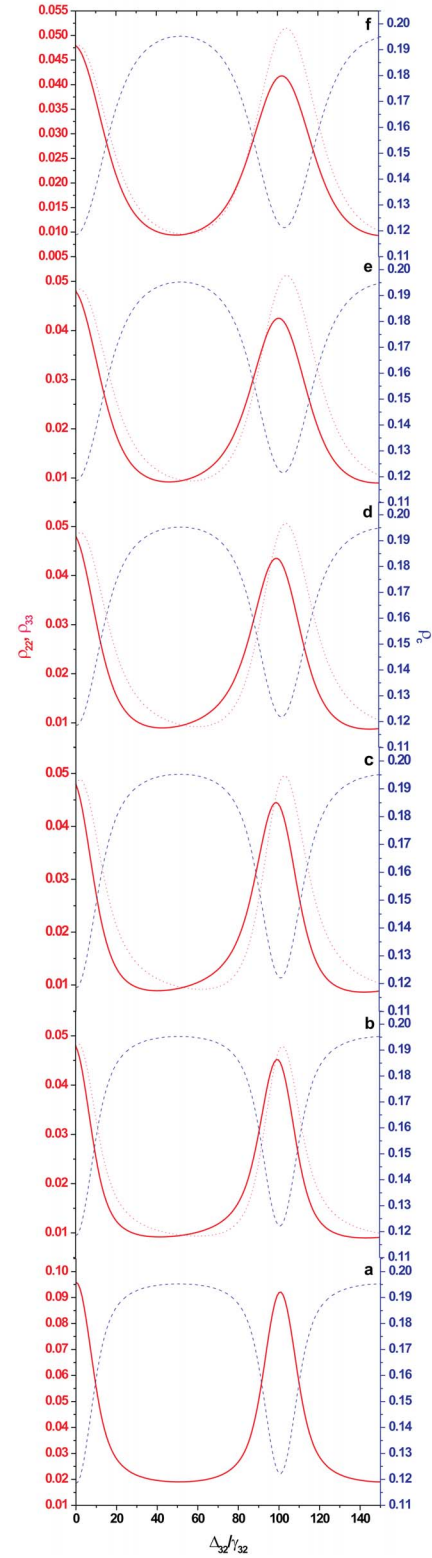


FIG. 7. (Color online) Populations of the metastable Zeeman sublevels ( $\rho_{22}$  shown by the solid and  $\rho_{33}$  by the dotted line, respectively) and in the continuum (dashed line) in the case of nonzero  $q$ . Pulse train parameters are the same as in Fig. 4, number of pulses in the train  $N=11$ ; for different  $q$ : (a)  $q=0$ , (b)  $q=0.5$ , (c)  $q=1$ , (d)  $q=1.5$ , (e)  $q=2$ , (f)  $q=2.5$ .

dressed in the present work is interaction with multiple spin-orbit continua. The details of this interaction and the strengths of the transitions to the continua will be the subject of another paper.

#### IV. CONCLUSIONS

We have theoretically analyzed the coherent population trapping effect with a train of ultrashort pulses coupling two bound states to a continuum of states in a  $\Lambda$ -type configuration. Complete ionization suppression can be realized in this system if the splitting between bound states is a multiple of the pulse repetition rate  $\Delta=2\pi n/T$ . In a traditional case with only two fields, pump and probe, complete ionization suppression cannot take place due to incoherent losses, induced by the two fields interacting with both bound states. Natural cancellation of incoherent ionization losses in CPT with a pulse train can be of great benefit for all LISC and coherent control experiments, leading to less background and better controllability. In fact, interaction of a train of pulses with a diatomic molecule was predicted to lead to efficient coherent control of quantum chaotic diffusion in this system [35]. A possibility of using CPT with a train of pulses technique to suppress ESA of pumping radiation into the conduction band of laser crystals is discussed. A specific example of  $\text{Ti}^{3+}:\text{YAlO}_3$  crystal, promising tunable yellow-orange laser,

is numerically studied. More than an order of magnitude enhancement of pumping efficiency is predicted in the two-photon resonance situation  $\Delta=2\pi n/T$  compared to the far-from-resonance pumping  $\Delta \neq 2\pi n/T$ . This enhancement takes place under pumping with ultrashort pulses with spectral width exceeding the Zeeman splitting and it is most effective if the train duration is of the order of the Zeeman coherence decay time. It also requires strong coupling of both Zeeman sublevels to the same continuum, and thus spin-orbit mixing of continuum states and, probably, some specific polarization of the pumping light to control interaction with multiple continua. If realized, the  $\text{Ti}^{3+}:\text{YAlO}_3$  laser can find numerous applications as a substitute for dye lasers in, for example, laser medical research, astronomy, navigation, and other areas. Due to the wide emission band ( $\sim 3000 \text{ cm}^{-1}$ ) of  $\text{Ti}^{3+}:\text{YAlO}_3$  it can be used for generation of ultrashort pulses utilizing some kind of mode-locking technique in the same way as the Ti:sapphire laser is used.

#### ACKNOWLEDGMENTS

The authors gratefully acknowledge financial support from NSF and AFOSR and wish to thank Anne Matsuura, Jack Agee, Marlan Scully, and Yuri Rostovtsev for stimulating and helpful discussions.

- 
- [1] P. L. Knight, M. A. Lauder, and B. J. Dalton, *Phys. Rep.* **190**, 1 (1990).
- [2] U. Fano, *Phys. Rev.* **124**, 1866 (1961).
- [3] T. Halfmann, L. P. Yatsenko, M. Shapiro, B. W. Shore, and K. Bergmann, *Phys. Rev. A* **58**, R46 (1998); L. P. Yatsenko, T. Halfmann, B. W. Shore, and K. Bergmann, *ibid.* **59**, 2926 (1999).
- [4] K. Böhmer, T. Halfmann, L. P. Yatsenko, D. Charalambidis, A. Horsmans, and K. Bergmann, *Phys. Rev. A* **66**, 013406 (2002).
- [5] A. Shnitman, I. Sofer, I. Golub, A. Yogev, M. Shapiro, Z. Chen, and P. Brumer, *Phys. Rev. Lett.* **76**, 2886 (1996); M. Shapiro and P. Brumer, *Rep. Prog. Phys.* **66**, 859 (2003).
- [6] T. Peters, L. P. Yatsenko, and T. Halfmann, *Phys. Rev. Lett.* **95**, 103601 (2005).
- [7] S. E. Harris, *Part. Sci. Technol.* **50**, 36 (1997); M. Fleischhauer, A. Imamoglu, and J. P. Marangos, *Rev. Mod. Phys.* **77**, 633 (2005).
- [8] E. Arimondo, in *Progress in Optics*, edited by E. Wolf (Elsevier Science, Amsterdam, 1996), Vol. 35, pp. 257–354.
- [9] A. B. Matsko, O. Kocharovskaya, Y. Rostovtsev, G. R. Welch, A. S. Zibrov, and M. O. Scully, *Adv. At., Mol., Opt. Phys.* **46**, 191 (2001).
- [10] K. Bergmann, H. Theuer, and B. W. Shore, *Rev. Mod. Phys.* **70**, 1003 (1998).
- [11] S. Kück, *Appl. Phys. B: Lasers Opt.* **72**, 515 (2001).
- [12] E. Kuznetsova, R. Kolesov, and O. Kocharovskaya, *Phys. Rev. A* **70**, 043801 (2004); R. Kolesov, E. Kuznetsova, and O. Kocharovskaya, *Phys. Rev. A* **71**, 043815 (2005).
- [13] O. A. Kocharovskaya and Ya. I. Khanin, *Sov. Phys. JETP* **63**, 945 (1986).
- [14] V. A. Sautenkov, Y. V. Rostovtsev, C. Y. Ye, G. R. Welch, O. Kocharovskaya, and M. O. Scully, *Phys. Rev. A* **71**, 063804 (2004).
- [15] R. Kolesov, *Phys. Rev. A* **72**, 051801(R) (2005).
- [16] L. Arissian, J. Jones, and J.-C. Diels, *J. Mod. Opt.* **49**, 2517 (2002).
- [17] F. Renzoni, A. Lindner, and E. Arimondo, *Phys. Rev. A* **60**, 450 (1999).
- [18] E. Paspalakis, M. Protopapas, and P. L. Knight, *J. Phys. B* **31**, 775 (1998).
- [19] H. M. Pask, *Prog. Quantum Electron.* **27**, 3 (2003).
- [20] V. V. Ter-Mikirtychev and T. Tsuboi, *Prog. Quantum Electron.* **3**, 219 (1996).
- [21] J. Kvapil, M. Koselja, J. Kvapil, B. Perner, V. Skoda, J. Kubelka, *J. Phys. B* **38**, 237 (1988).
- [22] M. Yamaga, B. Henderson, and K. P. O'Donnell, *Appl. Phys. B: Photophys. Laser Chem.* **52**, 122 (1991).
- [23] M. Yamaga, B. Henderson, K. P. O'Donnell, F. Rasheed, Y. Gao, and B. Cockayne, *Appl. Phys. B: Photophys. Laser Chem.* **52**, 225 (1991).
- [24] A. Abragam and B. Bleaney, *Electron Paramagnetic Resonance of Transition Ions* (Clarendon Press, Oxford, 1970).
- [25] J. H. Van Vleck, *Phys. Rev.* **57**, 426 (1940).
- [26] S. A. Basun, T. Danger, A. A. Kaplyanskii, D. S. McClure, K. Petermann, and W. C. Wong, *Phys. Rev. B* **54**, 6141 (1996).

- [27] M. Yamaga, T. Yosida, B. Henderson, K. P. O'Donnell, and M. Date, *J. Phys.: Condens. Matter* **4**, 7285 (1992).
- [28] J.-P. Meyn, T. Danger, K. Petermann, and G. Huber, *J. Lumin.* **55**, 55 (1993).
- [29] M. A. Noginov, G. B. Loutts, D. E. Jones, V. J. Turney, R. R. Rakhimov, L. Herbert, and A. Truong, *J. Appl. Phys.* **91**, 569 (2002).
- [30] T. Wegner and K. Petermann, *Appl. Phys. B: Photophys. Laser Chem.* **49**, 275 (1989).
- [31] S. Cavalieri, R. Eramo, L. Fini, M. Materazzi, O. Faucher, and D. Charalambidis, *Phys. Rev. A* **57**, 2915 (1998).
- [32] T. Nakajima and L. A. A. Nikolopoulos, *Phys. Rev. A* **68**, 013413 (2003).
- [33] J. C. Hensel and K. Suzuki, *Phys. Rev. Lett.* **22**, 838 (1969).
- [34] M. Willatzen, M. Cardona, and N. E. Christensen, *Phys. Rev. B* **51**, 17992 (1995).
- [35] J. Gong and P. Brumer, *Annu. Rev. Phys. Chem.* **56**, 1 (2005).